A Method of Analysis of TE_{11}-to-HE_{11} Mode Converters

LUIZ C. DA SILVA

Abstract—**An efficient method for the determination of the scattering matrix of TE_{11}-to-HE_{11} corrugated cylindrical waveguide mode converters has been developed based on the representation of the fields inside the corrugations by a small number of radial waveguide modes. Numerical results show that the method, when compared to the usual mode-matching techniques, reduces the computation time, without loss of accuracy.**

I. Introduction

THE TRANSITION FROM a smooth to a corrugated cylindrical waveguide in corrugated horns is usually accomplished by TE_{11}-to-HE_{11} mode converters, consisting of a nonuniform corrugated waveguide with several sections, as shown in Fig. 1. The main objectives in the design of the converter are to obtain a low SWR in the smooth waveguide and to avoid the generation of unwanted modes in the corrugated horn.

Design criteria have been established elsewhere [1]–[7] and will not be discussed here.

For analyzing the performance of these devices, several approximate techniques have been developed. Dragone [1] applied a simplified impedance model to the corrugated waveguide section and obtained simple expressions for the reflection and transmission coefficients. Cooper [8] modeled the converter as a transition between a smooth-walled and a uniform corrugated waveguide, and used mode-matching techniques in the determination of the propagation behavior of the structure. Daniele *et al.* [9] employed a similar model, but applied the the Winer–Hopf method to their analysis. Navarro *et al.* [10] characterized a rectangular corrugated waveguide as a smooth waveguide periodically loaded with infinitely thin irises, and determined the propagation constants of the waveguide using a network analysis. Their model can be adapted to circular waveguides.

The approximate techniques cited above are very useful as a tool in the initial steps of the design. More accurate methods of analysis, however, are necessary to give an accurate prediction of the behavior of broad-band converters.

An accurate analysis can be done by applying mode-matching techniques in the computation of the scattering matrices for each discontinuity in waveguide cross section of the converter, and for each section of smooth waveguide separating them. By progressively cascading the partial scattering matrices, an overall scattering matrix is obtained [4]. Some computer time can be saved if the scattering matrices of each module, composed of two adjacent sections of waveguide, are calculated directly [11].

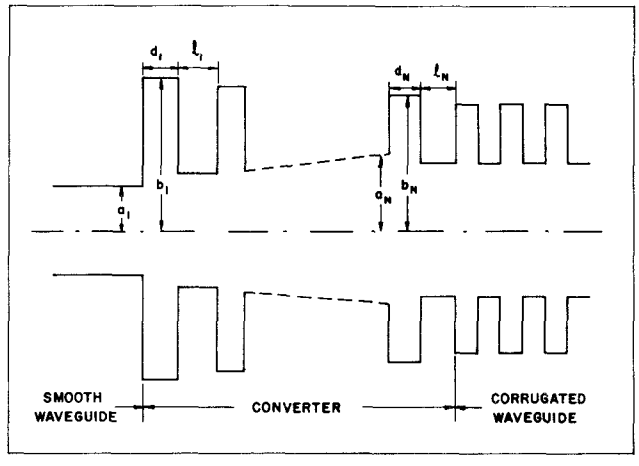

Fig. 1. Cross section of a mode converter.

The cascading process can be stopped at a section where the remainder of the horn can be considered as formed by a homogeneous currugated waveguide [4]. The adequacy of the choice of this section can be verified by checking the convergence of the results as more sections are included in the computation. Alternatively, all corrugations of the horn can be included in determining the scattering matrix. In this case, the solutions for the fields interior and exterior to the horn must be matched [11].

The main drawback of the above method is the large number of modes frequently necessary to represent the fields in the waveguide sections, and the resulting time involved in the computations.

In the present paper an alternative method for the determination of the scattering matrix of TE_{11}-to-HE_{11} cylindrical waveguide converters is presented that is able to reduce the computation time without loss of accuracy. Such time reduction is achieved by the utilization of radial waveguide modes in the characterization of the fields inside the corrugations. Since such modes, with exception of the TM_{01}, are highly evanescent, a few are enough to represent the fields. In fact, numerical results show that, for the cases of interest, convergence is achieved with only three radial modes.

Manuscript received February 9, 1987; revised September 15, 1987. This work was supported in part by TELEBRÁS S. A. (Brazilian Telecommunications Agency).

The author is with the Pontificia Universidade Catolica do Rio de Janeiro, Rua Marques de Sao Vicente, 225-Gavea, 22453 Rio de Janeiro, Brazil

IEEE Log Number 8718371.

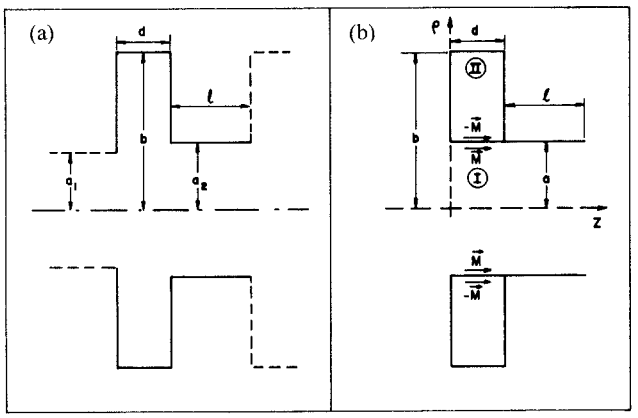

Fig. 2. The unit cell of the converter. (a) The original unit cell. (b) The equivalent unit cell.

II. Formulation

The scattering matrix of the converter will be determined from unit cells, as shown in Fig. 2(a). It will be assumed initially that $a_1 = a_2 = a$, and the cell of Fig. 2(a) will be transformed into the equivalent structure of Fig. 2(b), where a metallic wall and equivalent magnetic surface currents, $-\vec{M}$ and $\vec{M}$ were placed between the corrugation and the smooth waveguide.

The magnetic surface current $\vec{M}$, according to the equivalence principle [12], is given by

$$\vec{M} = \vec{a}_\rho \times \vec{E}_A \tag{1}$$

where $\vec{a}_\rho$ is the unit vector in the ρ direction, and $\vec{E}_A$ is the electric field effectively existing at $\rho = a$, $0 \leqslant z \leqslant d$. In this way, the unit cell is decomposed into two regions: region I corresponding to a smooth waveguide section of radius a and length $d + l$, and region II corresponding to a cylindrical cavity defined by the surfaces $\rho = a$, $\rho = b$, $z = 0$, and $z = d$. It will be assumed that in region I there is an incident wave, propagating along the positive z direction, and given by a summation of TE_{1n} and TM_{1n} modes for the waveguide of radius a. The magnetic fields in regions I and II must satisfy the following boundary condition at $\rho = a$:

$$\vec{H}^T_{\text{cav}}(a) = \vec{H}^T_{\omega g}(a) + \vec{H}^T_{in}(a) \tag{2}$$

where $\vec{H}^T_{\omega g}(a)$ and $\vec{H}^T_{\text{cav}}(a)$ are the components transverse to $\vec{a}_\rho$ of the magnetic fields generated by $[\pm]\,\vec{M}$ in regions I and II, respectively, and $\vec{H}^T_{in}(a)$ is the component transverse to $\vec{a}_\rho$ of the magnetic field of the incident wave.

$\vec{H}^T_{\omega g}(a)$ and $\vec{H}^T_{\text{cav}}(a)$ can be determined from the magnetic dyadic Green's functions for regions I and II:

$$\vec{H}_{\omega g}(\vec{r}) = \int \bar{\bar{G}}_{\text{I}}(\vec{r}, \vec{r}') \cdot \vec{M}\, ds' \tag{3a}$$

$$\vec{H}_{\text{cav}}(\vec{r}) = -\int \bar{\bar{G}}_{\text{II}}(\vec{r}, \vec{r}') \cdot \vec{M}\, ds' \tag{3b}$$

where $\bar{\bar{G}}_{\text{I}}$ and $\bar{\bar{G}}_{\text{II}}$ are the magnetic dyadic Green's functions for regions I and II, and $\vec{r}$ and $\vec{r}'$ are the position vectors of the observation and source points, respectively. Analytical expressions for $\bar{\bar{G}}_{\text{I}}$ and $\bar{\bar{G}}_{\text{II}}$ are given in Appendix I.

The magnetic surface current $\vec{M}$ can be expressed as

$$\vec{M} = \sum_{n=1}^{NE+NM} \vec{M}_n \tag{4}$$

where $\vec{M}_n$ is the component of $\vec{M}$ due to the mode $(1, n)$ of the incident wave and NE $[NM]$ is the number of TE [TM] modes considered in region I, which must be large enough to ensure convergence.

$\vec{M}_n$, according to (1), can be put into the form

$$\vec{M}_n = \sum_{p=0}^{PM} m^M_{pn} \vec{a}_\rho \times \vec{e}^{\text{TM}}_p + \sum_{p=1}^{PE} m^E_{pn} \vec{a}_\rho \times \vec{e}^{\text{TE}}_p \tag{5}$$

where $\vec{e}^{\text{TE}}_p$ $[\vec{e}^{\text{TM}}_p]$ is the electric field of the radial TE_{p1} $[TM_{p1}]$ mode for the parallel-plate radial waveguide of region II at $\rho = a$; PE $[PM+1]$ is the number of radial TE [TM] modes considered in region II; and m^M_{pn} and m^E_{pn} are coefficients to be determined.

Applying (A2), (4), and (5) in (3b) and performing the indicated integration, the following results are obtained.

$$\vec{H}^T_{\text{cav}}(a) = \sum_{n=1}^{NE+NM} \sum_{p=0}^{PM} m^M_{pn} \vec{H}^M_p + \sum_{n=1}^{NE+NM} \sum_{p=1}^{PE} m^E_{pn} \vec{H}^E_p \tag{6a}$$

where

$$\vec{H}^M_p = -j\omega\epsilon_0 C^M_p \sin\phi \cos\alpha_p z \vec{a}_\phi \tag{6b}$$

$$\vec{H}^E_p = -\frac{1}{j\omega\mu_0} C^E_p \left(\frac{\alpha_p}{a} \sin\phi \cos\alpha_p z \vec{a}_\phi - k^2_{\rho_p} \cos\phi \sin\alpha_p z \vec{a}_z \right) \tag{6c}$$

$$C^M_p = \frac{H^{(2)}_1(k_{\rho_p} b) J'_1(k_{\rho_p} a) - J_1(k_{\rho_p} b) H^{(2)\prime}_1(k_{\rho_p} a)}{J_1(k_{\rho_p} b) H^{(2)}_1(k_{\rho_p} a) - J_1(k_{\rho_p} a) H^{(2)}_1(k_{\rho_p} b)} \tag{6d}$$

$$C^E_p = \frac{H^{(2)}_1(k_{\rho_p} a) J'_1(k_{\rho_p} b) - H^{(2)\prime}_1(k_{\rho_p} b) J_1(k_{\rho_p} a)}{J'_1(k_{\rho_p} b) H^{(2)\prime}_1(k_{\rho_p} a) - J'_1(k_{\rho_p} a) H^{(2)\prime}_1(k_{\rho_p} b)} \tag{6e}$$

$$k_{\rho_p} = \sqrt{k_0^2 - \alpha_p^2} \tag{6f}$$

$$\alpha_p = p\pi/d. \tag{6g}$$

Here ϵ_0 is the free-space permitivity; μ_0 is the free-space permeability; $J_1(x)$ is the Bessel function of the first kind of order 1; $H^{(2)}_1(x)$ is the Hankel function of the second kind of order 1; $J'_1(kx) = d[J_1(kx)]/dx$; $H^{(2)\prime}_1(kx) = d[H^{(2)}_1(kx)]/dx$; and ρ, ϕ, and z are the cylindrical coordinates of a point in the coordinate system shown in Fig. 2(b).

In the same way, (3a), (A1), (4), and (5) yield

$$\begin{aligned} \vec{H}^T_{\omega g}(a) = &\sum_{n'=1}^{NE+NM} \sum_{p=1}^{PE} m^E_{pn'} \left(\sum_{n=1}^{NE} \vec{h}^{\text{TE-TE}}_{pn} \right) \\ &+ \sum_{n'=1}^{NE+NM} \sum_{p=0}^{PM} m^M_{pn'} \left(\sum_{n=1}^{NE} \vec{h}^{\text{TE-TM}}_{pn} \right) \\ &+ \sum_{n'=1}^{NE+NM} \sum_{p=0}^{PM} m^M_{pn'} \left(\sum_{n=1}^{NM} \vec{h}^{\text{TM-TM}}_{pn} \right). \end{aligned} \tag{7}$$

The superscript TE[TM] − TE[TM] on the vectors $\vec{h}^{\text{TE-TE}}_{pn}$, $\vec{h}^{\text{TE-TM}}_{pn}$, and $\vec{h}^{\text{TM-TM}}_{pn}$ refers to the component of the magnetic field in the mode $TE_{1n}[TM_{1n}]$ for the smooth

waveguide produced by the component of the surface magnetic current associated to the radial mode $TE_{p1}[TM_{p1}]$ for the parallel-plate radial waveguide. The components ϕ and z of these vectors have the general form

$$h^{x-y}_{\alpha_{pn}} = \gamma^{x-y}_{\alpha_n}\left[q^{x-y}_{\alpha_{pn}}e^{j\alpha_p z} + r^{x-y}_{\alpha_{pn}}e^{-j\alpha_p z} + s^{x-y}_{\alpha_{pn}}e^{j\beta_n z} + t^{x-y}_{\alpha_{pn}}e^{-j\beta_n z}\right]\begin{cases}\sin\phi & \text{if } \alpha=\phi\\ \cos\phi & \text{if } \alpha=z\end{cases} \quad (8)$$

where β_n is the propagation constant of the mode $(1,n)$ for region I, x and y mean TE or TM, and α means ϕ or z. The expressions for the constants $\gamma^{x-y}_{\alpha_n}$, $q^{x-y}_{\alpha_{pn}}$, $r^{x-y}_{\alpha_{pn}}$, $s^{x-y}_{\alpha_{pn}}$, and $t^{x-y}_{\alpha_{pn}}$ are given in Table I. In this table, $k^{TE}_{c_n}$ $[k^{TM}_{c_n}]$ and β^{TE}_n $[\beta^{TM}_n]$ are the cutoff wavenumber and propagation constant, respectively, of the TE_{1n} $[TM_{1n}]$ mode in region I.

Substituting (6) and (7) into (2), vector multiplying both members of the resulting equation by $\vec{e}^{TE}_p$, $p=1,2,\cdots,PE$, and $\vec{e}^{TM}_p$, $p=0,1,2,\cdots,PM$, and integrating both members of the resulting expression over the surface $\rho=a$, $0\leq z\leq d$, the following system of linear equations is obtained:

$$\left[\overline{\overline{Q}}\right]\begin{bmatrix}\overline{\overline{M}}_E\\ \overline{\overline{M}}_m\end{bmatrix} = \left[\overline{\overline{H}}_{in}\right]. \quad (9)$$

Here $\overline{\overline{Q}}$ is a matrix $(PE+PM+1)\times(PE+PM+1)$; $\overline{\overline{M}}_E$ and $\overline{\overline{M}}_m$ are matrices $PE\times(NE+NM)$ and $(PM+1)\times(NE+NM)$, respectively, containing the coefficients m^E_{pn} and m^M_{pn}; and $\overline{\overline{H}}_{in}$ is a matrix $(PE+PM+1)\times(NE+NM)$. Expressions for the elements of $\overline{\overline{Q}}$ and $\overline{\overline{H}}_{in}$ are given in Appendix II.

The solution of the system of equations (9) yields the values of the coefficients m^E_{pn} and m^M_{pn}. It should be observed that the matrix to be inverted in the solution of this system is of small dimension (the number of radial modes, $PE+PM+1$, necessary to ensure convergence of

TABLE I
EXPRESSIONS FOR THE COEFFICIENTS $\gamma^{x-y}_{\alpha_n}$, $q^{x-y}_{\alpha_{pn}}$, $r^{x-y}_{\alpha_{pn}}$, $s^{x-y}_{\alpha_{pn}}$, AND $t^{x-y}_{\alpha_{pn}}$

COMPONENT	VECTOR	γ_{α_n}	$q^{x-y}_{\alpha_{pn}}$	$r^{x-y}_{\alpha_{pn}}$	$s^{x-y}_{\alpha_{pn}}$	$t^{x-y}_{\alpha_{pn}}$
ϕ	$\vec{h}^{TE-TE}$	$\dfrac{j\,k^{TE^2}_{c_n}}{2\,\omega\mu_o[(k^{TE}_{c_n}a)^2-1]}$	$\dfrac{2\,\alpha_p}{\alpha_p^2-\beta^{TE^2}_n}$	$=q_{np}$	$-\left[\dfrac{e^{j(\alpha_p-\beta^{TE}_n)d}}{\alpha_p-\beta^{TE}_n}+\dfrac{e^{-j(\alpha_p+\beta^{TE}_n)d}}{\alpha_p+\beta^{TE}_n}\right]$	$=-q_{np}$
	$\vec{h}^{TE-TM}$	$\dfrac{1}{2j\,\omega\mu_o a[(k^{TE}_{c_n}a)^2-1]}$	$\dfrac{2(\beta^{TE^2}_n k^2_{\rho_p}-\alpha_p^2 k^{TE^2}_{c_n})}{\alpha_p^2-\beta^{TE^2}_n}$	$=q_{np}$	$\dfrac{e^{j(\alpha_p-\beta^{TE}_n)d}}{\alpha_p-\beta^{TE}_n}(\alpha_p k^{TE^2}_{c_n}-\beta^{TE}_n k^2_{\rho_p})+\dfrac{e^{-j(\alpha_p+\beta^{TE}_n)d}}{\alpha_p+\beta^{TE}_n}(\alpha_p k^{TE^2}_{c_n}+\beta^{TE}_n k^2_{\rho_p})$	$\dfrac{2(k^{TE^2}_{c_n}\alpha_p^2-\beta^{TE^2}_n k^2_{\rho_p})}{\alpha_p^2-\beta^{TE^2}_n}$
	$\vec{h}^{TM-TM}$	$\dfrac{-\omega\varepsilon_o}{2j\,a\,\beta^{TM}_n}$	$\dfrac{-2\,\beta^{TM}_n k^2_{\rho_p}}{\alpha_p^2-\beta^{TM^2}_n}$	$=q_{np}$	$k^2_{\rho_p}\left[\dfrac{e^{j(\alpha_p-\beta^{TM}_n)d}}{\alpha_p-\beta^{TM}_n}-\dfrac{e^{-j(\alpha_p+\beta^{TM}_n)d}}{\alpha_p+\beta^{TM}_n}\right]$	$=-q_{np}$
z	$\vec{h}^{TE-TE}$	$\dfrac{k^{TE^4}_{c_n}a}{2\,\omega\mu_o\beta^{TE}_n[(k^{TE}_{c_n}a)^2-1]}$	$-\dfrac{2\,\beta^{TE}_n}{\alpha_p^2-\beta^{TE^2}_n}+\dfrac{2\,\beta^{TE}_n}{k^{TE^2}_{c_n}}$	$=-q_{np}$	$\dfrac{e^{j(\alpha_p-\beta^{TE}_n)d}}{\alpha_p-\beta^{TE}_n}+\dfrac{e^{-j(\alpha_p+\beta^{TE}_n)d}}{\alpha_p+\beta^{TE}_n}$	$\dfrac{-2\,\alpha_p}{\alpha_p^2-\beta^{TE^2}_n}$
	$\vec{h}^{TE-TM}$	$\dfrac{k^{TE^2}_{c_n}}{2\,\omega\mu_o[(k^{TE}_{c_n}a)^2-1]}$	$\dfrac{2\,\alpha_p(k^2_{\rho_p}-k^{TE^2}_{c_n})}{\alpha_p^2-\beta^{TE^2}_n}+2\alpha_p$	$=-q_{np}$	$\dfrac{e^{j(\alpha_p-\beta^{TE}_n)d}k^{TE^2}_{c_n}}{\alpha_p-\beta^{TE}_n}(\dfrac{\alpha_p}{\beta^{TE}_n}-k^2_{\rho_p})+\dfrac{e^{-j(\alpha_p+\beta^{TE}_n)d}k^{TE^2}_{c_n}}{\alpha_p+\beta^{TE}_n}(\dfrac{\alpha_p}{\beta^{TE}_n}+k^2_{\rho_p})$	$\dfrac{2(\beta^{TE}_n k^2_{\rho_p}-k^{TE^2}_{c_n}\alpha_p^2/\beta^{TE}_n)}{\alpha_p^2-\beta^{TE^2}_n}$

the results, is small), and consequently the inversion process is very fast.

Once m_{pn}^{E} and m_{pn}^{M} are known, the elements of the scattering matrix of the unit cell can be determined, as shown in the next section.

III. The Scattering Matrix of a Unit Cell

Let us consider the unit cell divided into two sections: section A going from $z=0$ to $z=d$ and section B going from $z=d$ to $z=d+l$. The scattering matrix of section A, due to its symmetry, can be expressed as

$$\left[\bar{\bar{S}}^{a}\right]=\begin{bmatrix}\bar{\bar{S}}_{11}^{a} & \bar{\bar{S}}_{21}^{a}\\ \bar{\bar{S}}_{21}^{a} & \bar{\bar{S}}_{11}^{a}\end{bmatrix}. \tag{10}$$

$\bar{\bar{S}}_{11}^{a}$ and $\bar{\bar{S}}_{21}^{a}$ are matrices $(NE+NM)\times(NE+NM)$, with elements defined by

$$s_{11_{i,j}}^{a}=\frac{V_{1i}^{-}}{V_{1j}^{+}} \tag{11a}$$

$$s_{21_{i,j}}^{a}=\frac{V_{2i}^{-}}{V_{1j}^{+}} \tag{11b}$$

where V_{1i}^{-} $[V_{1j}^{+}]$ is the amplitude of the reflected [incident] magnetic field component in the $(1,i)$ $[1,j]$ mode of the smooth waveguide of radius a, defined at $z=0$, and V_{2i}^{-} is the amplitude of the transmitted magnetic field component in the $(1,i)$ mode, defined at $z=d$.

Applying (3a), (A1), (4), and (5) in the determination of V_{1i}^{-}/V_{1j}^{+} and V_{2i}^{-}/V_{1j}^{+}, we obtain

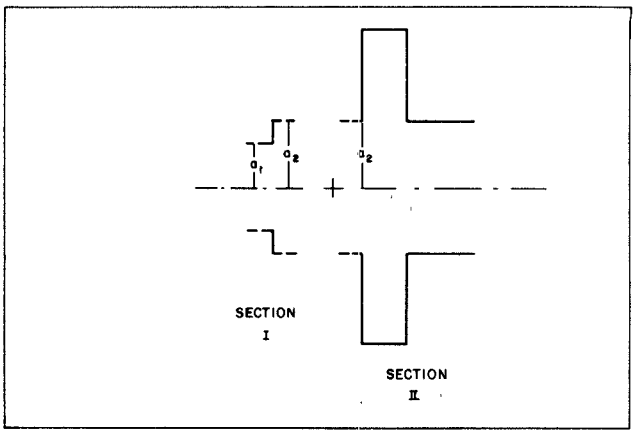

Fig. 3. Decomposition of the unit cell if $a_1 \neq a_2$.

where

$$F_1(a,b)=\frac{1}{2j}\int_0^d e^{jbz}\cos az\,dz \tag{13a}$$

$$F_2(a,b)=-\frac{1}{2}\int_0^d e^{jbz}\sin az\,dz \tag{13b}$$

$$\delta_{i,j}=\begin{cases}1 & \text{if } i=j\\ 0 & \text{if } i\neq j.\end{cases}$$

Section B is a smooth waveguide of radius a and length l, with a scattering matrix given by

$$\bar{\bar{S}}^{b}=\begin{bmatrix}\bar{\bar{S}}_{11}^{b} & \bar{\bar{S}}_{21}^{b}\\ \bar{\bar{S}}_{21}^{b} & \bar{\bar{S}}_{11}^{b}\end{bmatrix} \tag{14}$$

where $\bar{\bar{S}}_{11}^{b}=0$ and $s_{21_{i,j}}^{b}=\exp(-j\beta_i l)\delta_{ij}$.

$$s_{11_{i,j}}^{a}=\frac{-a}{2j\beta_i^{\mathrm{TE}}\left[\left(k_{c_i}^{\mathrm{TE}}a\right)^2-1\right]J_1\left(k_{c_i}^{\mathrm{TE}}a\right)}\cdot\left\{\sum_{p=1}^{PE}m_{pj}^{E}k_{c_i}^{\mathrm{TE}^2}F2\left(\alpha_p,-\beta_i^{\mathrm{TE}}\right)\right.$$

$$\left.+\sum_{p=0}^{PM}m_{pj}^{M}\left[-\frac{k_{\rho_p}^2\beta_i^{\mathrm{TE}}}{a}F_1\left(\alpha_p,-\beta_i^{\mathrm{TE}}\right)+\frac{\alpha_p k_{c_i}^{\mathrm{TE}^2}}{a}F_2\left(\alpha_p,-\beta_i^{\mathrm{TE}}\right)\right]\right\}\cdots\begin{cases}i=1, & NE\\ j=1, & NE+NM\end{cases} \tag{12a}$$

$$s_{11_{i+NE,j}}^{a}=\frac{j\omega\epsilon_0}{2\beta_i^{\mathrm{TM}}aJ_1'\left(k_{c_i}^{\mathrm{TM}}a\right)}\sum_{p=0}^{PM}m_{pj}^{M}k_{\rho_p}^2F_1\left(\alpha_p,-\beta_i^{\mathrm{TM}}\right)\cdots\begin{cases}i=1, & NM\\ j=1, & NE+NM\end{cases} \tag{12b}$$

$$s_{21_{i,j}}^{a}=e^{-j\beta_i^{\mathrm{TE}}d}\left\{\frac{-a}{2j\beta_i^{\mathrm{TE}}\left[\left(k_{c_i}^{\mathrm{TE}}a\right)^2-1\right]J_1\left(k_{c_i}^{\mathrm{TE}}a\right)}\right\}\left\{\sum_{p=1}^{PE}m_{pj}^{E}k_{c_i}^{\mathrm{TE}^2}F_2\left(\alpha_p,\beta_i^{\mathrm{TE}}\right)+\sum_{p=0}^{PM}m_{pj}^{M}\left[\frac{k_{\rho_p}^2\beta_i^{\mathrm{TE}}}{a}F_1\left(\alpha_p,\beta_i^{\mathrm{TE}}\right)\right.\right.$$

$$\left.\left.+\frac{\alpha_p k_{c_i}^{\mathrm{TE}^2}}{a}F_2\left(\alpha_p,\beta_i^{\mathrm{TE}}\right)\right]\right\}+e^{-j\beta_i^{\mathrm{TE}}d}\delta_{i,j}\cdots\begin{cases}i=1, & NE\\ j=1, & NE+NM\end{cases} \tag{12c}$$

$$s_{21_{i+NE,j}}^{a}=\frac{-j\omega\epsilon_0}{2\beta_i^{TM}aJ_1'\left(k_{c_i}^{TM}a\right)}\sum_{p=0}^{PM}m_{pj}^{M}k_{\rho_p}^2F_1\left(\alpha_p,\beta_i^{\mathrm{TM}}\right)\Big)e^{-j\beta_i^{\mathrm{TM}}d}+e^{-j\beta_i^{\mathrm{TM}}d}\delta_{i+NE,j}\cdots\begin{cases}i=1, & NM\\ j=1, & NE+NM\end{cases} \tag{12d}$$

TABLE II
DIMENSIONS (IN cm) OF THE WAVEGUIDE SECTION (INCLUDING A SEVEN-SECTION CONVERTER) OF THE CORRUGATED HORN USED IN MEASUREMENTS

i	a_i	a_{i+1}	b_i	d_i	ℓ_i	OBS
1	1.34	1.34	3.34	0.20	0.38	
2	1.34	1.34	3.20	0.20	0.34	
3	1.34	1.34	3.05	0.20	0.30	
4	1.34	1.34	2.91	0.20	0.26	Mode converter
5	1.34	1.34	2.77	0.20	0.22	
6	1.34	1.34	2.63	0.20	0.18	
7	1.34	1.34	2.48	0.20	0.14	
8 to 10	1.34	1.34	2.34	0.20	0.10	

Cascading the scattering matrices of sections A and B (applying eq. (1) of [13]), we obtain, finally, the scattering matrix of the unit cell:

$$\bar{\bar{S}}_{11} = \bar{\bar{S}}^a_{11} \tag{15a}$$

$$\bar{\bar{S}}_{12} = \bar{\bar{S}}^a_{21}\bar{\bar{S}}^b_{21} \tag{15b}$$

$$\bar{\bar{S}}_{21} = \bar{\bar{S}}^b_{21}\bar{\bar{S}}^a_{21} \tag{15c}$$

$$\bar{\bar{S}}_{22} = \bar{\bar{S}}^b_{21}\bar{\bar{S}}^a_{11}\bar{\bar{S}}^b_{21}. \tag{15d}$$

The above expressions are valid if the input and output radii of the unit cell, a_1 and a_2, are equal. If $a_1 \neq a_2$, the unit cell is decomposed into two cascaded sections, as shown in Fig. 3. The scattering matrix of section I, a discontinuity in waveguide radius, is calculated according to [4] (since the radius discontinuity, $a_2 - a_1$, is usually small, the number of modes used in this calculation will not be very large). Section II corresponds to a unit cell with inner waveguide of constant radius, as considered before.

The overall scattering matrix of the converter is obtained by progressively cascading the scattering matrices of its unit cells.

IV. EXPERIMENTAL AND NUMERICAL RESULTS

As a test of validity of the method of analysis, measurements were made in a corrugated horn, composed of a section of nonhomogeneous waveguide, plus a flared section, with a semiflare angle of 11°, corrugations 10.0 mm in depth, a length of 2.0 mm, and a distance between corrugations of 3.0 mm. The diameter of the aperture is 18.5 cm. The dimensions of the waveguide section, which includes a seven-section converter plus three corrugations, are given in Table II.

Measured and theoretical results for the return loss are shown in Fig. 4. Computations were made by cascading 21 corrugations and approximating the remainder of the horn by a homogeneous corrugated waveguide of infinite length. A total of 24 longitudinal modes and three radial modes were used at the first corrugation. Theoretical results, calculated according to [4], are also shown in Fig. 4 (22 modes were used at the input waveguide).

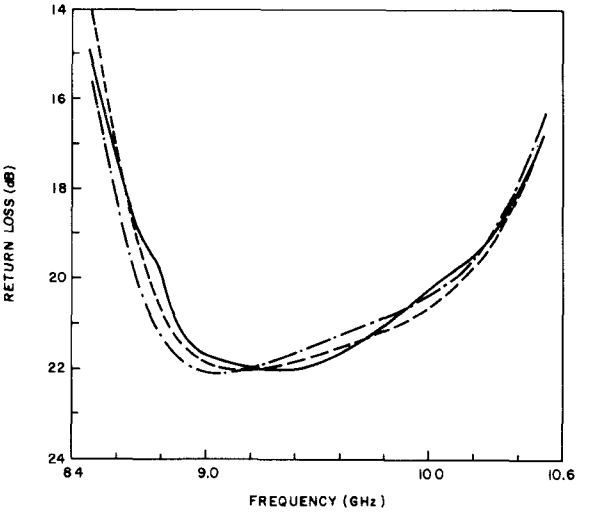

Fig. 4. Return loss, as a function of frequency, of the corrugated horn described in the text, with the converter dimensions shown in Table II. (——) Experimental results; (----) theoretical results applying the method proposed in this paper; (–·–·–) theoretical results applying the method proposed in [4].

Discrepancies between experimental and theoretical results are less than 1.2 dB. Discrepancies between the two theoretical results are less than 0.5 dB, except at the lower end of the frequency band, where a value of 1.5 dB is obtained. Computations using radial modes, however, were three times faster.

The convergence of the results, as a function of the number of radial modes and longitudinal modes considered, is shown in Tables III and IV, respectively.

TABLE III
CONVERGENCE OF THE RETURN LOSS AS A FUNCTION OF THE NUMBER OF RADIAL MODES CONSIDERED IN THE COMPUTATIONS (32 LONGITUDINAL MODES WERE USED IN THE LAST SECTION)

Nº of Radial Modes / Freq.	1	2	3	4	5	6	7
8.6	17.1	16.4	17.4	17.4	17.2	17.1	17.1
9.0	22.7	21.6	22.1	22.0	22.0	21.9	22.0
10.0	20.1	21.0	20.5	20.5	20.6	20.6	20.5

TABLE IV
CONVERGENCE OF THE RETURN LOSS AS A FUNCTION OF THE NUMBER OF LONGITUDINAL MODES CONSIDERED IN THE COMPUTATION (THREE RADIAL MODES WERE USED)

Nº of Longitudinal Modes / Freq.	8	12	16	20	24	28	32	36
8.6	15.0	15.1	15.3	16.5	16.9	17.2	17.4	17.4
9.0	20.7	21.3	21.6	21.9	21.9	22.0	22.1	22.0
10.0	21.0	20.9	20.9	20.7	20.6	20.6	20.5	20.5

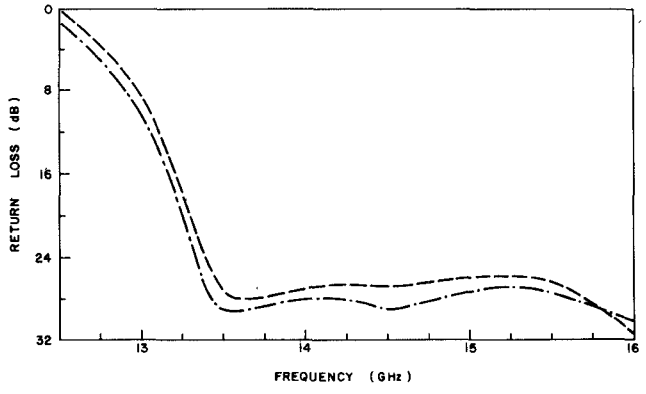

Fig. 5. Return loss, as a function of frequency, of the converter configuration of [4, fig. 5]. (---) Present method; (-·-·-) method of [4].

It is observed that three radial modes and 24 longitudinal modes, at the first corrugation, were enough to ensure convergence.

If the number of cascaded corrugations used in the computations is increased (a smaller section of the horn is approximated by a corrugated waveguide), fluctuations of about 1 dB appear in the results. This is a limitation on the accuracy of the method, unless all corrugations are taken into consideration, as suggested in [11].

As a second example of numerical results, Fig. 5 shows the return loss of the converter configuration of [4, fig. 5] applying, again, the method proposed in this paper (using 16 longitudinal modes and two radial modes) and in [4] (14 modes at the input waveguide). Results agree within 2 dB. Computer time using radial modes was four times smaller.

V. CONCLUSIONS

An efficient and accurate method for the determination of the scattering matrix of TE_{11}-to-HE_{11} mode converters was presented, based on the application of equivalent surface magnetic currents and on the representation of the fields inside the corrugations by a small number of radial modes.

Due to the computer time economy resulting from the utilization of the method, it can be used to advantage in analyzing the performance of corrugated horns.

APPENDIX I
THE MAGNETIC DYADIC GREEN'S FUNCTIONS FOR REGIONS I AND II

The development of the magnetic dyadic Green's functions for regions I and II will follow the procedure given in [14]. Since in this reference the field sources considered are electric current densities, the duality principle will be applied to adapt the results to magnetic current densities.

Region I is a circular waveguide of radius a, and its magnetic dyadic Green's function can be taken directly from [14, eq. (59)]:

$$\bar{\bar{G}}_I = u(z-z')\sum_n \frac{\vec{h}_n^{>}(\vec{r})\vec{h}_n^{<}(\vec{r}')}{2Y_n} + u(z'-z)\sum_n \frac{\vec{h}_n^{<}(\vec{r})\vec{h}^{>}(\vec{r}')}{2Y_n} - \frac{\vec{a}_z\vec{a}_z}{j\omega\mu_0}\delta(\vec{r}-\vec{r}') \quad \text{(A1)}$$

where $u(z-z')$ is the Heaviside unit step function $u(\epsilon)$,

defined by

$$u(\epsilon) = \begin{cases} 1, & \epsilon > 0 \\ 0, & \epsilon < 0. \end{cases}$$

Here $\delta(\vec{r}, \vec{r}')$ is the Dirac delta function, $\vec{r}$ [$\vec{r}'$] is the position vector of the observation [source] point, Y_n is the wave admittance of the mode n, and $\vec{h}_n^{>}(\vec{r})$ [$\vec{h}_n^{<}(\vec{r})$] are the modal magnetic fields for propagation in the positive [negative] z direction, TE and TM to z (given by [12, eqs. (5.18), (5.19), (5.23), and (5.27)].

Region II is a waveguide cavity limited by the surfaces $\rho = a$, $\rho = b$, $z = 0$, and $z = d$. Its magnetic dyadic Green's function can be expressed as [14]

$$\overline{\overline{G}}_{\mathrm{II}} = \overline{\overline{G}}_{\omega\mathrm{II}} + \sum_p \vec{h}_p^{<}(\vec{r})\left[C_{p1}\vec{h}_p^{>}(\vec{r}') + D_{p1}\vec{h}_p^{<}(\vec{r}')\right] + \sum_p \vec{h}_p^{>}(r)\left[C_{p2}\vec{h}_p^{>}(\vec{r}') + D_{p2}\vec{h}_p^{<}(\vec{r}')\right] \quad \text{(A2)}$$

where $\overline{\overline{G}}_{\omega\mathrm{II}}$ is the magnetic dyadic Green's function for the parallel-plate waveguide formed by the surfaces $z = 0$ and $z = d$; C_{p1}, C_{p2}, D_{p1}, and D_{p2} are coefficients to be determined; and $\vec{h}_p^{>}(\vec{r})$ [$\vec{h}_p^{<}(\vec{r})$] are the magnetic modal fields for the parallel-plate waveguide, for propagation along the positive [negative] ρ direction, TE and TM to ρ (given by [12, eqs. (5.18), (5.19), (5.33), and (5.35)]).

$\overline{\overline{G}}_{\omega\mathrm{II}}$, like $\overline{\overline{G}}_{\mathrm{I}}$, can be put into the form

$$\overline{\overline{G}}_{\omega\mathrm{II}} = u(\rho - \rho')\sum_p \frac{\vec{h}_p^{>}(\vec{r})\vec{h}_p^{<}(\vec{r}')}{Y_p} + u(\rho' - \rho)\sum_p \frac{\vec{h}_p^{<}(\vec{r})\vec{h}_p^{>}(\vec{r}')}{Y_P} - \frac{\vec{a}_\rho \vec{a}_\rho}{j\omega\mu_0}\delta(\vec{r} - \vec{r}') \quad \text{(A3)}$$

where

$$Y_p = \int_{\phi=0}^{2\pi}\int_{z=0}^{d}\left|\vec{e}_p^{<} \times \vec{h}_p^{>} - \vec{e}_p^{>} \times \vec{h}_p^{<}\right| \cdot \vec{a}_\rho \rho \, d\phi \, dz = \begin{cases} k_{\rho_p}^2 d/\omega\mu_0 & \text{for TE modes} \\ -k_{\rho_p}^2 d(1+\delta_p)/\omega\epsilon_0 & \text{for TM modes} \end{cases}$$

$$\delta_p = \begin{cases} 1 & \text{if } p = 0 \\ 0 & \text{if } p \neq 0. \end{cases}$$

C_{p1}, C_{p2}, D_{p1}, and D_{p2} are obtained from the application of the boundary conditions at $\rho = a$ and $\rho = b$:

$$\vec{a}_\rho \times \left(\nabla \times \overline{\overline{G}}_{\mathrm{II}}\right)\Big|_{\rho=a}^{\rho=b} = 0. \quad \text{(A4)}$$

Substituting (A2) and (A3) into (A4) gives for TE (to ρ) modes,

$$C_{p1} = \frac{J_1'(k_{\rho_p}a)H_1^{(2)'}(k_{\rho_p}b)}{Y_n\left[J_1'(k_{\rho_p}b)H_1^{(2)'}(k_{\rho_p}a) - J_1'(k_{\rho_p}a)H_1^{(2)'}(k_{\rho_p}b)\right]} \quad \text{(A5)}$$

$$C_{p2} = -\frac{J_1'(k_{\rho_p}b)}{H_1^{(2)'}(k_{\rho_p}b)}C_{p1} \quad \text{(A6)}$$

$$D_{p1} = \frac{H_1^{(2)'}(k_{\rho_p}b)H_1^{(2)'}(k_{\rho_p}a)}{Y_n\left[J_1'(k_{\rho_p}b)H_1^{(2)'}(k_{\rho_p}a) - J_1'(k_{\rho_p}a)H_1^{(2)'}(k_{\rho_p}b)\right]} \quad \text{(A7)}$$

$$D_{p2} = -\frac{J_1'(k_{\rho_p}a)}{H_1^{(2)'}(k_{\rho_p}a)}D_{p1}.$$

For TM modes, the functions $J_1'(x)$ and $H_1'^{(2)}(x)$ must be replaced by $J_1(x)$ and $H_1^{(2)}(x)$ in the above expressions.

Appendix II
Expressions for the Elements of the Matrices $\overline{\overline{Q}}$ and $\overline{\overline{H}}_{in}$

The elements of the matrices $\overline{\overline{Q}}$ and $\overline{\overline{H}}_{in}$ [eq. (9)], are obtained by vector multiplying both members of (2) by $\vec{e}_i^{\,\mathrm{TE}}$, $i = 1, 2, \cdots, PE$, and $\vec{e}_i^{\,\mathrm{TM}}$, $i = 0, 1, 2, \cdots, PM$, and integrating the resulting expression over the surface $\rho = a$, $0 \leq z \leq d$:

$$\int\left[\vec{e}_i^{\,\mathrm{TE[TM]}} \times \vec{H}_{\omega g}^{T}(a)\right] \cdot \vec{a}_\rho \, ds - \left[\vec{e}_i^{\,\mathrm{TE[TM]}} \times \vec{H}_{\mathrm{cav}}^{T}(a)\right] \cdot \vec{a}_\rho \, ds = -\int\left[\vec{e}_i^{\,\mathrm{TE[TM]}} \times \vec{H}_{in}^{T}(a)\right] \cdot \vec{a}_\rho \, ds, \quad i = 1, PE[i = 0, PM] \quad \text{(A8)}$$

where $\vec{e}_i^{\,\mathrm{TE[TM]}}$ is the modal electric field of the radial $\mathrm{TE}_{i1}[\mathrm{TM}_{i1}]$ mode for the parallel-plate waveguide of region II; $\vec{H}_{in}^{T}(a)$ is the component transverse to $\vec{a}_\rho$ of the magnetic field of the incident wave; and $\vec{H}_{\mathrm{cav}}^{T}(a)$ and $\vec{H}_{\omega g}^{T}(a)$ are given by (6) and (7), respectively.

Performing the operations indicated in (A8), we obtain

$$\sum_{j=1}^{PE} q_{ij}m_{ij}^{E} + \sum_{j=0}^{PM} q_{i,j+PE+1}m_{ij}^{M} = \sum_{n=1}^{NE+NM} h_{in_{1,n}}, \quad i = 1, PE + PM + 1 \quad \text{(A9)}$$

where

$$q_{i,j} = \sum_{n=1}^{NE} \gamma_{z_n}^{\mathrm{TE-TE}} F_2 T\left(\alpha_i, \alpha_j, \beta_n^{\mathrm{TE}}, q_{z_{jn}}^{\mathrm{TE-TE}}, r_{z_{jn}}^{\mathrm{TE-TE}}, s_{z_{jn}}^{\mathrm{TE-TE}}, t_{z_{jn}}^{\mathrm{TE-TE}}\right) - dk_{\rho_i}^2 C_i^E \delta_{i,j} \cdots \begin{cases} i = 1, & PE \\ j = 1, & PE \end{cases} \quad \text{(A10)}$$

$$q_{i,j+PE+1} = \sum_{n=1}^{NE} \gamma_{z_n}^{\mathrm{TE-TM}} F_2 T\left(\alpha_i, \alpha_j, \beta_n^{\mathrm{TE}}, q_{z_{jn}}^{\mathrm{TE-TM}}, r_{z_{jn}}^{\mathrm{TE-TM}}, s_{z_{jn}}^{\mathrm{TE-TM}}, t_{z_{jn}}^{\mathrm{TE-TM}}\right) \cdots \begin{cases} i = 1, & PE \\ j = 0, & PM \end{cases} \quad \text{(A11)}$$

$$q_{i+PE+1,j} = -\frac{\alpha_i}{a}\sum_{n=1}^{NE}\gamma_{z_n}^{TE-TE}F_2T\left(\alpha_i,\alpha_j,\beta_n^{TE},q_{z_{jn}}^{TE-TE},r_{z_{jn}}^{TE-TE},s_{z_{jn}}^{TE-TE},t_{z_{jn}}^{TE-TE}\right)$$

$$-jk_{\rho_i}^2\sum_{n=1}^{NE}\gamma_{\phi_n}^{TE-TE}F_1T\left(\alpha_i,\alpha_j,\beta_n^{TE},q_{\phi_{jn}}^{TE-TE},r_{\phi_{jn}}^{TE-TE},s_{\phi_{jn}}^{TE-TE},t_{\phi_{jn}}^{TE-TE}\right)\cdots\begin{cases}i=0, & PM\\ j=1, & PE\end{cases} \tag{A12}$$

$$q_{i+PE+1,j+PE+1} = -\frac{\alpha_i}{a}\sum_{n=1}^{NE}\gamma_{z_n}^{TE-TM}F_2T\left(\alpha_i,\alpha_j,\beta_n^{TE},q_{jn}^{TE-TM},r_{z_{jn}}^{TE-TM},s_{z_{jn}}^{TE-TM},t_{z_{jn}}^{TE-TM}\right)$$

$$-jk_{\rho_i}^2\sum_{n=1}^{NE}\gamma_{\phi_n}^{TE-TM}F_1T\left(\alpha_i,\alpha_j,\beta_n^{TE},q_{\phi_{jn}}^{TE-TM},r_{\phi jn}^{TE-TM},s_{\phi_{jn}}^{TE-TM},t_{\phi_{jn}}^{TE-TM}\right)$$

$$-jk_{\rho_i}^2\sum_{n=1}^{NM}\gamma_{\phi_n}^{TM-TM}F_1T\left(\alpha_i,\alpha_j,\beta_n^{TM},q_{\phi_{jn}}^{TM-TM},r_{\phi_{jn}}^{TM-TM},s_{\phi_{jn}}^{TM-TM},t_{\phi_{jn}}^{TM-TM}\right)$$

$$-k_{\rho_i}^2 dC_i^M(1+\delta_i)\delta_{i,j}\begin{cases}i=0, & PM\\ j=0, & PM\end{cases} \tag{A13}$$

$$h_{in_{i,j}} = -\frac{1}{j\omega\mu_0}k_{c_j}^{TE^2}J_1\left(k_{c_j}^{TE}a\right)F_2\left(\alpha_i,-\beta_j^{TE}\right)\cdots\begin{cases}i=1, & PE\\ j=1, & NE\end{cases} \tag{A14}$$

$$h_{in_{i,j+NE}} = 0\begin{cases}i=1, & PE\\ j=1, & NM\end{cases} \tag{A15}$$

$$h_{in_{i+PE+1,j}} = \frac{J_1\left(k_{c_j}^{TE}a\right)}{j\omega\mu_0 a}\left[\alpha_i k_{c_j}^{TE^2}F_2\left(\alpha_i,-\beta_j^{TE}\right)-k_{\rho_i}^2\beta_j^{TE}F_1\left(\alpha_i-\beta_j^{TE}\right)\right]$$

$$\cdots\begin{cases}i=0, & PM\\ j=1, & NE\end{cases} \tag{A16}$$

$$h_{in_{i+PE+1,j+NE}} = -jJ_1'\left(k_{c_i}^{TM}a\right)k_{\rho_i}^2F_1\left(\alpha_i,-\beta_i^{TM}\right)\cdots\begin{cases}i=0, & PM\\ j=1, & NM\end{cases}. \tag{A17}$$

The functions $F_1T(\alpha_i,\alpha_j,\beta,q,r,s,t)$ and $F_2T(\alpha_i,\alpha_j,\beta,q,r,s,t)$ are defined as

$$F_1T = qF_1(\alpha_i,\alpha_j)+rF_1(\alpha_i,-\alpha_j)+sF_1(\alpha_i,\beta)+tF_1(\alpha_i,-\beta)$$

$$F_2T = qF_2(\alpha_1,\alpha_j)+rF_2(\alpha_i,-\alpha_j)+sF_2(\alpha_i,\beta)+tF_2(\alpha_i,-\beta).$$

$F_1(a,b)$ and $F_2(a,b)$ are given by (13a) and (13b); the parameters q, r, s, t and γ are given in Table I; C_i^E and C_i^M are given by (6d) and (6e), respectively; and the other symbols are as defined before.

ACKNOWLEDGMENT

The author is indebted to Prof. A. R. Panicali and Dr. S. Ghosh for their useful suggestions.

REFERENCES

[1] C. Dragone, "Reflection, transmission, and mode conversion in a corrugated feed," *Bell Syst. Tech. J.*, vol. 56, no. 6, pp. 835–867, July–Aug. 1977.

[2] C. Dragone, "Characteristics of a broadband microwave corrugated feed: A comparison between theory and experiment," *Bell Syst. Tech. J.*, vol. 56, no. 6, pp. 869–888, July–Aug. 1977.

[3] C. Dragone, and W. E. Legg, "Quarter-wave corrugated transformer for broadband matching of a corrugated feed," *Bell Syst. Tech. J.*, vol. 63, no. 2, pp. 207–215, Feb. 1984.

[4] G. L. James, "Analysis and design of TE_{11}-to-HE_{11} corrugated cylindrical waveguide mode converters," *IEEE Trans. Microwave Theory Tech.*, vol. MTT-29, pp. 1059–1066, 1981.

[5] G. L. James and B. M. Thomas, "TE_{11}-to-HE_{11} cylindrical waveguide mode converters using ring-loaded slots," *IEEE Trans. Microwave Theory Tech.*, vol. MTT-30, pp. 278–285, Mar. 1982.

[6] B. M. Thomas, "Mode conversion using circumferentially corrugated cylinrical waveguide," *Electron. Lett.*, vol. 8, pp. 394–396, July 1972.

[7] S. F. Mahmoud, "Mode conversion on profiled corrugated conical horns," *Proc. Inst. Elec. Eng.*, vol. 130, pt. H, no. 6, pp. 415–419, Oct. 1983.

[8] D. N. Cooper, "Complex propagation coefficients and the step discontinuity in corrugated cylindrical waveguides," *Electron. Lett.*, vol. 7, pp. 135–136, 1971.

[9] V. G. Daniele, I. Montrosset, and R. S. Zich, "Wiener–Hopf solution for the junction between a smooth and a corrugated cylindrical waveguide," *Radio Sci.*, vol. 14, pp. 943–955, 1979.

[10] M. S. Navarro, T. E. Rozzi and Y. T. Lo, "Propagation in a rectangular waveguide periodically loaded with resonant irises," *IEEE Trans. Microwave Theory Tech.*, vol. MTT-28, pp. 857–865, Aug. 1980.

[11] E. Kühn and V. Hombach, "Computer-aided analysis of corrugated horns with axial or ring-loaded radial slots," in *Proc. 3rd Int. Conf. Antennas Propagat.*, 1983, pp. 127–131.

[12] R. F. Harrington, *Time-Harmonic Electromagnetic Fields*. New York: McGraw-Hill, 1961.

[13] D. J. R. Stock and T. J. Kajdan, "A comment of the scattering matrix of cascaded $2n$-ports," *IRE Trans. Microwave Theory Tech.*, vol. MTT-9, pp. 54, Sept. 1961.

[14] P. H. Pathak, "On the eigenfunction expansion of electromagnetic dyadic Green's functions," *IEEE Trans. Antennas Propagat.*, vol. AP-31, pp. 837–846, 1983.

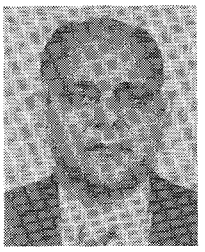

Luiz C. da Silva was born in Rio de Janeiro, Brazil, on October 11, 1936. He received the B.S. degree in electrical engineering from the Military Institute of Engineering, Brazil, in 1963, the M.Sc. degree from the Institute for Space Research, Brazil, in 1969, and the Ph.D. degree from the University of Illinois in 1974.

Since 1975 he has been engaged in research on reflector antennas and feeders as an Associate Professor at the Catholic University of Rio de Janeiro.